Available online at http://www.journalcra.com

International Journal of Current Research
Vol. 8, Issue, 12, pp.42815-42820, December, 2016

INTERNATIONAL JOURNAL OF CURRENT RESEARCH

ISSN: 0975-833X

RESEARCH ARTICLE

PREPARATION AND PHYSICO-CHEMICAL STUDY OF Mg DOPED $BaTiO_3$ ($Ba_{1-x}Mg_xTiO_3$) PREPARED BY THE SOL–GEL METHOD

[1, 2, *]Ouafae. El ghadraoui, [1]Mohammed. Zouhairi, [2,3]Farid.Abdi, [2]Taj-dine. Lamcharfi, [1]Hamza. Bali, [1]El houssine. El ghadraoui and [3]Michel. Aillerie

[1]Laboratoire de Chimie de la Matière Condensée, Université Sidi Mohammed Ben Abdellah, BP 2202, Route d'Imouzzer, Faculté des Sciences et Techniques de Fès, BP 2202, Fès, Morocco
[2]Laboratoire Signaux, Systèmes et Composants, Université Sidi Mohammed Ben Abdellah, BP 2202, Route d'Imouzzer, Faculté des Sciences et Techniques de Fès, BP 2202, Fès, Morocco
[3]Laboratoire Matériaux Optiques, Photonique et Systèmes, Université de Lorraine-Metz Supélec, 2 rue E. Belin, 57070 Metz, France

ARTICLE INFO

Article History:
Received 03rd September, 2016
Received in revised form
09th October, 2016
Accepted 15th November, 2016
Published online 30th December, 2016

Key words:

Perovskite, $Ba_{1-x}Mg_xTiO_3$,
XRD, Raman, Photoluminescence.

ABSTRACT

In this work the effect of doping with magnesium on the structural and physical properties of $BaTiO_3$ were studied. The ceramic materials of composition $Ba_{1-x}Mg_xTiO_3$ (x ranging from 0 to 1) were prepared by the sol-gel process at low sintering temperature (700°C). The results of XRD analysis showed a good incorporation of Mg in the BT structure for $x \leq 0,15$ and a mixture phases for $x > 0,15$, moreover, a photoluminescence spectra is observed for high Mg contents, while a flat response is obtained for $x \leq 0.15$.

Citation: Ouafae. El ghadraoui, Mohammed. Zouhairi, Farid.Abdi, Taj-dine. Lamcharfi, Hamza. Bali, El houssine. El ghadraoui and Michel. Aillerie, 2016. "Preparation and physico-chemical study of Mg doped $BaTiO_3$ ($Ba_{1-x}Mg_xTiO_3$) prepared by the sol–GEL method", *International Journal of Current Research*, 8, (12), 42815-42820.

INTRODUCTION

In recent years, much of the research activities have been conducted on ferroelectric materials because of their potential applications in various types of devices such as the storage information and Photonics electro-optic modulators and switches, actuators piezoelectric and infrared sensors (Uchino *et al.,* 1980; Swartz *et al.,* 1984). The perovskite ceramic materials such as $BaTiO_3$, $SrTiO_3$, $PbTiO_3$, $PbZr_xTi_{1-x}O_3$ (PZT) have been the subject numerous studies of their properties and particularly their ferroelectric character (Zouhairi thèse de doctorat, 2013; Zouhairi *et al.,* 2014). Some of them are now used in thin films for applications in microelectronics, FeRAM memories and other applications such as micro-actuators or displacement sensors because of their ferroelectricity and high dielectric and piezoelectric constants (Kang *et al.,* 2008; Asiaie *et al.,* 1996).

Corresponding author: Ouafae. El ghadraoui,
Laboratoire de Chimie de la Matière Condensée, Université Sidi Mohammed Ben Abdellah, BP 2202, Route d'Imouzzer, Faculté des Sciences et Techniques de Fès, BP 2202, Fès, Morocco.

$BaTiO_3$ has potential applications in photorefractive devices and memory storage, power electronic application and electro-optic devices (Kong *et al.,* 2002; Ohara *et al.,* 2008). Several changes to the BT composition have been studied to improve its physical properties to make it useful for applications (Tagantsev *et al.,* 2004). The aim of this work is the study of the effect of doping on this material. Moreover, the Mg doped BT ferroelectric material is an interesting candidate in phase shifters thanks its high dielectric nonlinearity and low dielectric loss (Cheng Liu *et al.,* 2011; Zimmermann *et al.,* 2012). BT shows three transitions depending on temperature: rhombohedral → orthorhombic → tetragonal → cubic. On an other hand, Magnesium titanate ($MgTiO_3$) is a ceramic oxide, characterized by a rhombohedral symmetry (ilmenite structure) with space group R3. This material is generally obtained by using solid-state reaction at very high sintering temperatures (T=1300°C). It has been extensively studied and used as a ceramic capacitor and resonator because of its low dielectric loss ($tg\delta \approx 10^{-4}$) and high thermal stability at high frequency. Since the methods of synthesis and doping or substitution are the key to improving the BT ceramic properties several synthesis methods were used to prepare a BT powder including

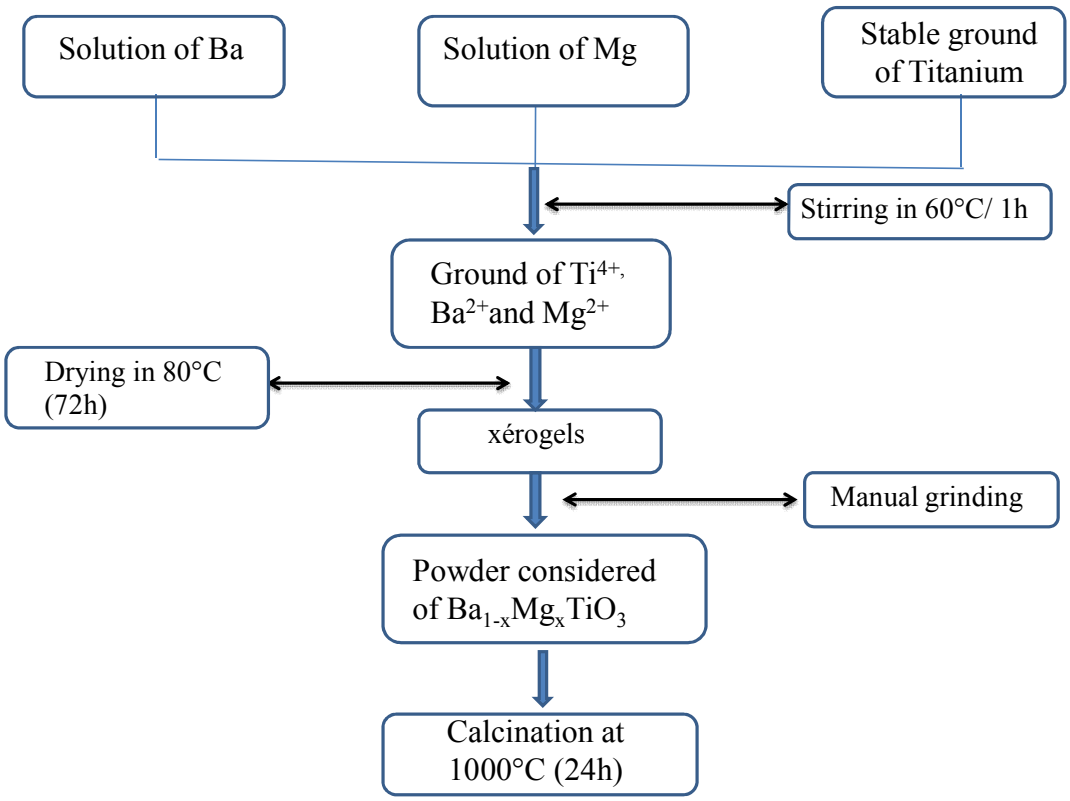

Figure 1. Illustration of the preparation of the $Ba_{1-x}Mg_xTiO_3$ ceramic by sol-gel method

non-conventional ones such as hydrothermal synthesis and polymer precursor method, mainly based on the Pechini type of process and sol-gel process (Kellati *et al.,* 2014; Bouayad *et al.,* 2005). The latter has many advantages as an excellent control of the stoichiometry, good homogeneity of the fine powder and low processing temperature (Harhira, 2007). The originality of the sol-gel process is to obtain, at low temperature (soft chemistry), a powder with generally amorphous structure powder which provides a ceramic by heat treatment. A new synthesis method allowed us to obtain pure compound at low temperature (T=700°C). The method of preparation of this material was the sol-gel process by means of the principle of the destabilization of colloidal solutions (DSC). The objective of this work is to study BM_xT powders prepared by using the sol-gel process. Powders having an Mg content varying from 0 to 100% have been characterized by X-ray diffraction, Raman spectroscopy and photoluminescence.

Experimental Procedure

In our preparation, $Ba_{1-x}Mg_xTiO_3$ were synthesized using magnesium acetate $Mg(CH_3COO)_2,3H_2O$, titanium alkoxide $Ti[OCH(CH_3)_2]_4$ and Barium acetate $(Ba(CH_3COO)_2$.The details of the preparation are shown in figure 1. For the preparation of titanium ground, an aqueous solution of lactic acid is stirred at 80°C for a few minutes. Then, the titanium alkoxide is added with carefully and rapidly to the mix, to avoid as much as possible the hydrolysis of the alkoxide (very sensitive to moisture). Molar ratios alkoxide/lactic acid and alkoxide/water were kept respectively equal to 2 and 1/33.33, to ensure high soil stability. The second step is to prepare a magnesium acetate solution. The third step is to prepare a solution of Barium acetate $(Ba(CH_3COO)_2)$.

A colloidal solution, was synthesized from titanate alkoxide $Ti[OCH(CH_3)_2]_4$ and lactic acid were stirred at 80°C for 24 h. The three solutions obtained are mixed in the following order: magnesium acetate, Barium acetate and titanium sol. These solutions are mixed in stochiometric proportions according to the chemical formulation $Ba_{1-x}Mg_xTiO_3$ stirring to ensure homogeneity of the solution. The destabilization of this solution is provided by evaporation of the solvent in an oven at a temperature of 80°C.

The solutions of $Ba_{1-x}Mg_xTiO_3$ dried in an oven lead to totally transparent xerogels after about 72 hours. The dry gel thus obtained is ground using an agate mortar to break up agglomerates of the powder and increase its reactivity. Raw powder obtained does not always crystallize in the desired perovskite phase, hence the need for calcining. The raw powder obtained after grinding in an agate mortar for 30 mn, is placed in an alumina boat, and then calcined in air, in a programmable oven. The calcination cycle adopted was chosen after several synthetic tests, slowly raising rate of 5°C/mn is necessary to prevent the ejection of the powder during the removal of organic matter especially acetates. A calcination step, for about one hour at 400°C is required for this operation. The temperature and the powder calcination time, at the second level required to obtain the desired phase, are generally defined after the heat study of the powder. The products were characterized by XRD, Raman measurements and photoluminescence were performed using a Raman spectrometer type Labram O10 (Jobin-Yvon) equipped with a CCD camera and a laser source He-Ne (633 nm) with a power rating of 15mW, an Argon laser source (514,5nm) to 20mW and a near-infrared laser source (785 nm), 40 mW.

RESULTS AND DISCUSSION

Analysis of the formed phases

Figure 2 shows the evolution of the formation at the BM_xT samples for $0 \leq x \leq 1$ sintered at 1000°C for 4 hours. Analysis of the various RX spectra obtained shows the appearance of three distinct domains. The first domain ranges from x=0 to 0.15, the second domain ranges from x=0.2 to 0.8 and the last domain for $x \geq 0.9$. Figure 3 shows spectra corresponding to the first domain (x=0, 0.5, 0.1, 0.15); these spectra are comparable to that of $BaTiO_3$. All lines of the spectra are perfectly indexed in a tetragonal structure. The XRD revealed that BMxT, ceramics crystallized into à single perovskite structure without changing the symmetry of the structure. These results indicate a good incorporation of Mg in BT structure. The Mg of smaller radius than Ba affects the lattice parameters, it is easily possible to observe the structural modification from tetragonal, as seen in figure 4, with the presence of two diffraction peaks (002) and (200) of undoped $BaTiO_3$ ceramic, to pseudo-cubic phase as the amount of magnesium is increased by merging the two diffraction peaks into one (200) and reducing the ratio c/a of tetragonality. (Table 1 and Figure 5).

Figure 6 shows the XRD patterns of BMxT ceramics, for x varying between 0.2 and 0.8. All the diffraction peaks, indicating the pseudocubic BMxT appeared in the patterns but with presence of the two secondary phases MgO and $BaMg_6Ti_6O_{19}$ (Jayanthi and Kutty, 2006) which proportion increase when the magnesium rate increases. We noted of the existence a chaotic domain due to the coexistence of secondary multiphases. The presence of secondary phase confirms the limit of solubility of Mg in the tetragonal phase of BT. This limit begins for x equal to 0.15. From 90% to 100% (figure 7), we notice the presence of two-phases, $MgTiO_3$ of rhombohedral symmetry and $BaTiO_3$ of pseudo cubic symmetry. The Barium of larger radius (r = 1.35Å), cannot replace Mg (r = 0.72 Å) in the crystallographic sites of the perovskite structure. The two-phases mixture, obtained, at x=0.9 are probably no purely phases, perhaps, Mg doped BT or Ba doped Mg. The cell parameters of $BMT_{0.15}$ are compared with pseudo cubic phase BT of the biphasic $BMT_{0.9}$ this is in good agree with the limit insertion the Mg in BT. The compared of pure $MgTiO_3$ parameters with the doped (x=0.9) shows a difference between parameters cell. This indicates that there is a little introduce of Ba into the $MgTiO_3$. For to confirm the Ba quantity inserted in $MgTiO_3$ others characterizations must be realized. For x=100%, the characteristic peaks of pure $MgTiO_3$ perovskite phase are observed.

Table 1. Tetragonality and cell volume, parameters for BM_xT heat treated at1000°C for 4h.

BM_xT	Parameters		Tetragonality	*c-a*(A°)	Cell Volume
x	*a* (A°)	*c* (A°)	*c/a*		$(A°)^3$
0	3.9983	4.0075	1.0023	0.0092	64.0655
0.05	4.0026	4.0092	1.0016	0.0066	64.2306
0.10	4.0054	4.0108	1.0013	0.0054	64.3461
0.15	4.0078	4.0115	1.0009	0.0037	64.4345
0.20	4.0085	4.0119	1.0008	0.0034	64.4635
0.25	4.0092	4.0124	1.0007	0.0032	64.4940
0.30	4.0099	4.0127	1.0006	0.0028	64.5214
0.90 (BT) (ThisWork)	4.0078	4.0102	1.0024	0.0024	64.4137
0.90 (MT)	5.133	12.821	2.5246	7.688	337.8037
PurMT	5.135	12.985	2.5189	7.85	342.3914

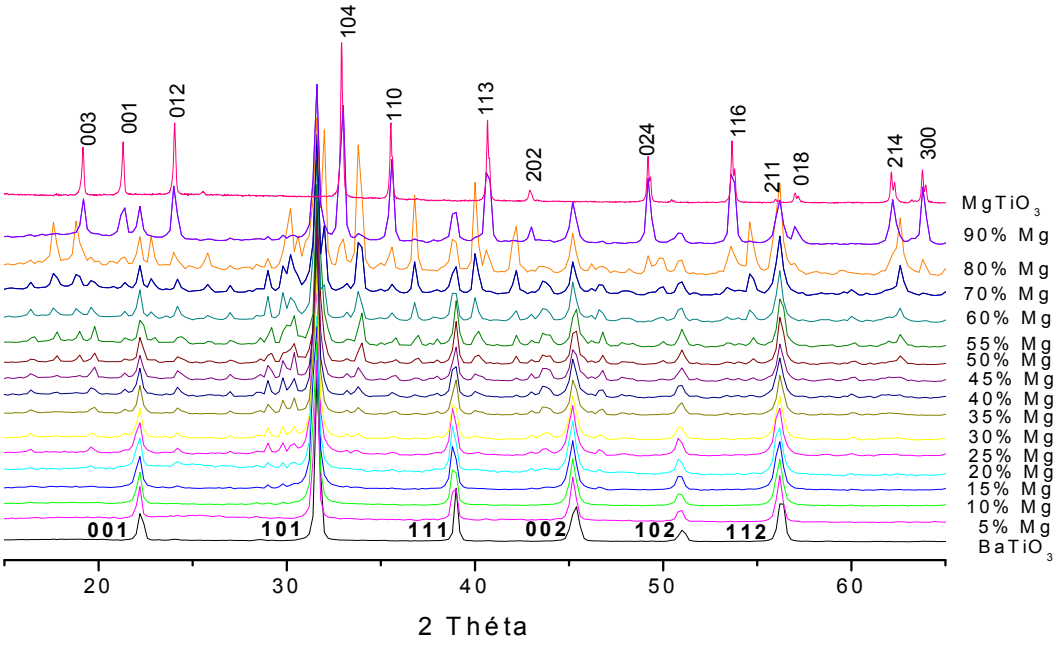

Figure 2. XRD spectra of the $Ba_{1-x}Mg_xTiO_3$ phases heat treated at 1000°C for 4h

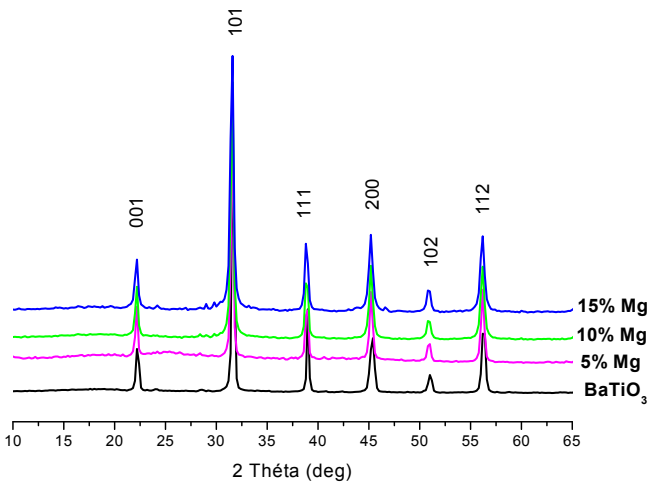

Figure 3: XRD spectra of $Ba_{1-x}Mg_xTiO_3$ ($0 \leq x \leq 0{,}15$) heat treated at 1000°C for 4h

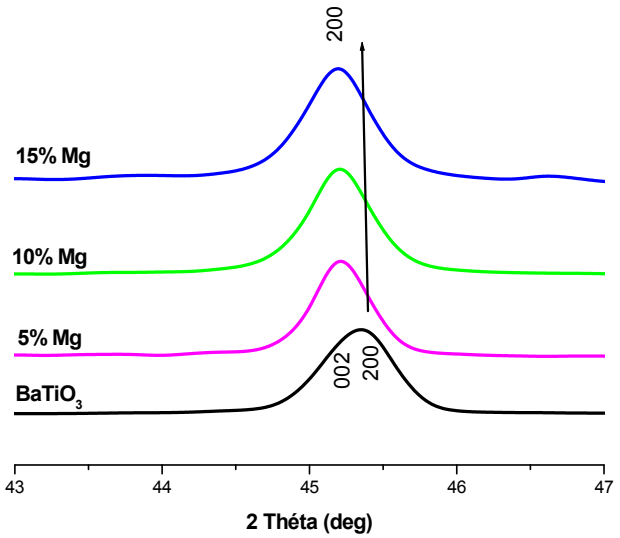

Figure 4. Zoom in of the gradual change from tetragonal is pseudo cubic structure

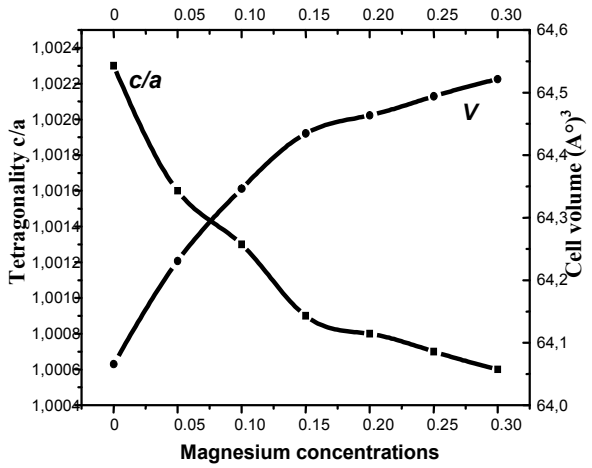

Figure 5. Evolution of tetragonality and cell volume of BMxT compounds

These results indicate that magnesium, with low rate ($x \leq 15\%$), is easily inserted into the tetragonal phase of BT without changing the symmetry of the structure. When the Mg content increases, the latter reacts with other elements to form secondary phases. The difference in symmetry between the two structures does not favour an incorporation of Mg. On the contrary, the Barium where law rate cannot be inserted in the $MgTiO_3$ rhombohedral symmetry.

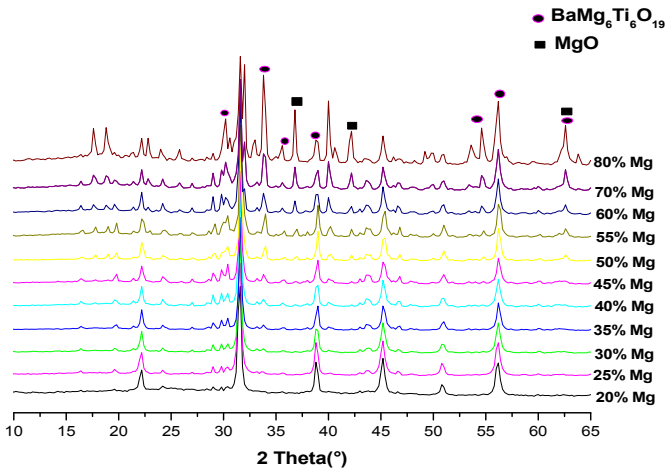

Figure 6. XRDof the $Ba_{1-x}Mg_xTiO_3$phases, with various magnesium concentrations ($0.2 \leq x \leq 0.8$) heat treated at 1000°C for 4h

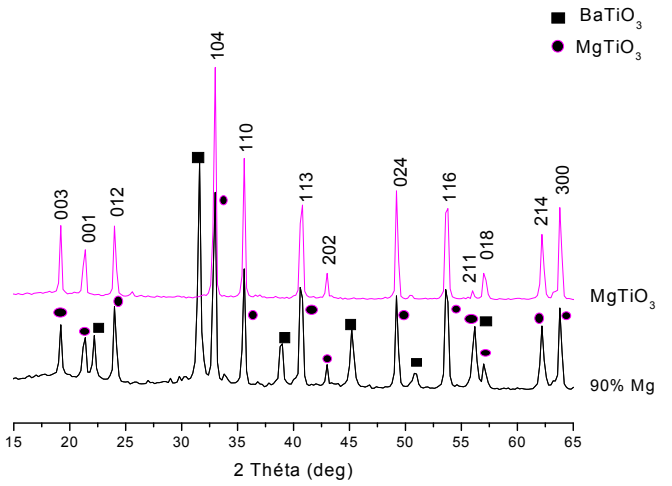

Figure 7. XRD spectraof$Ba_{1-x}Mg_xTiO_3$(x= 0.90 and 1) heat treated at 1000°C for 4h

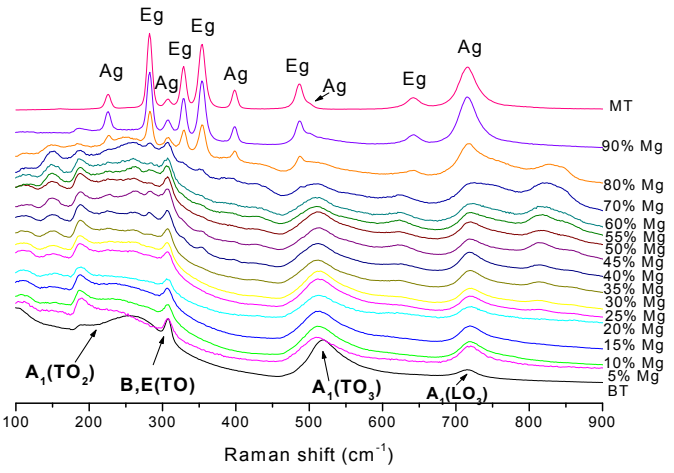

Figure 8. Raman Spectra of $Ba_{1-x}Mg_xTiO_3$ powders calcined at 1000°C for 4h

Raman spectroscopy: Figure 8 give the Raman spectra of various compounds of the solid solution $Ba_{1-x}Mg_xTiO_3$ in the frequency range of 100-900 cm^{-1}, it is observed the presence of three distinct domains, in accordance with a what was observed on XRD patterns. The Raman spectra obtained on BM_xT samples ($0 \leq x \leq 0.15$) are similar to that of pure BT confirming the tetragonal phase of these compounds and incorporation of Mg in the lattice (Figure 9).

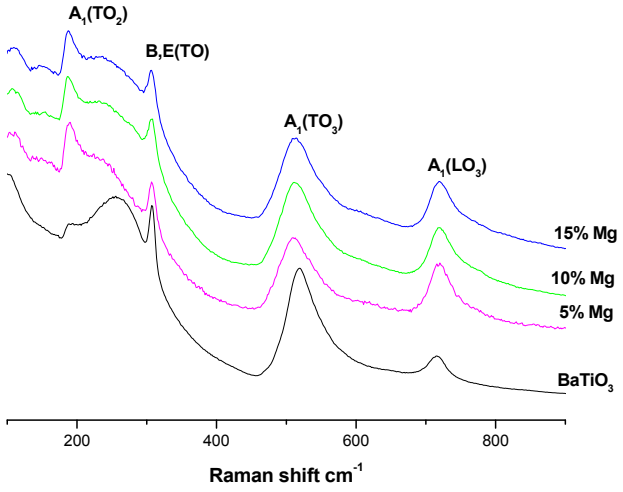

Figure 9. Raman spectra of $Ba_{1-x}Mg_xTiO_3$ ($0 \leq x \leq 0.15$)

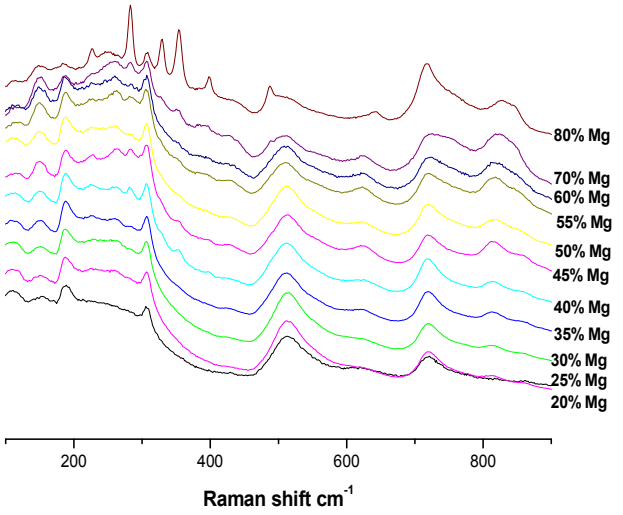

Figure 10.Raman spectra of $Ba_{1-x}Mg_xTiO_3$ ($0.20 \leq x\% \leq 0.80$)

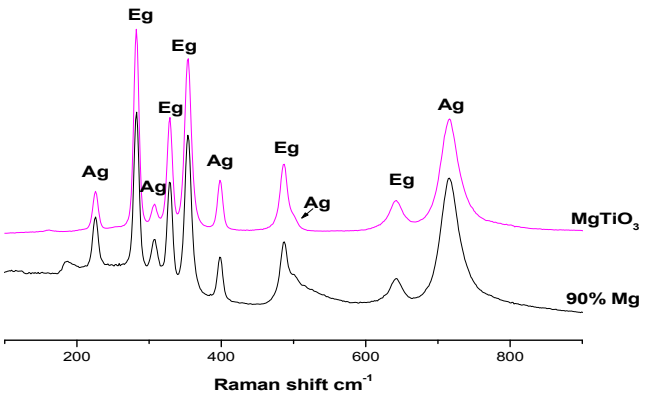

Figure 11. Raman spectra of $Ba_{1-x}Mg_xTiO_3$ (x= 0.9 and 1)

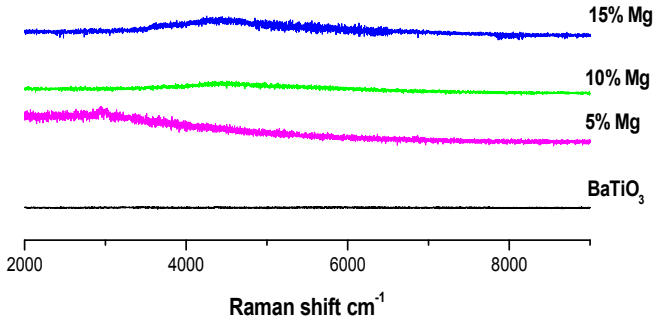

Figure 12. Photoluminescence spectra of $Ba_{1-x}Mg_xTiO_3$ ($0 \leq x \leq 15\%$)

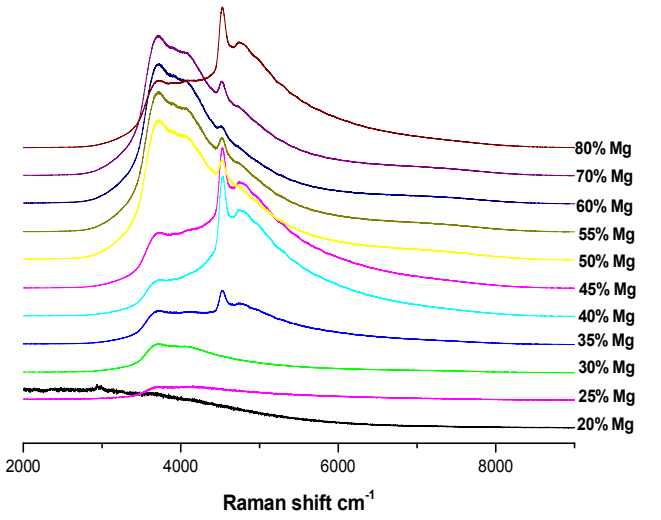

Figure 13. Photoluminescence spectra of $Ba_{1-x}Mg_xTiO_3$ ($20\% \leq x \leq 80\%$)

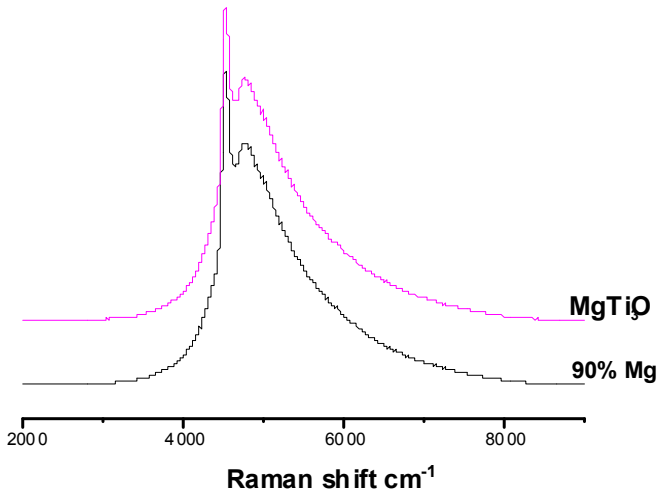

Figure 14. Photoluminescence spectra of $Ba_{1-x}Mg_xTiO_3$ (x =0.9 and 1)

On the spectrum of barium titanate (x=0), we observed a broad and asymmetric intense band due to the merging of modes A (TO1), A (LO1) and A (TO2) between 200 cm^{-1} and 280 cm^{-1}. It is also observes a narrow band at 310 cm^{-1} associated with modes B1, E (TO3 + LO2), and a broad and asymmetric band at 520 cm^{-1} associated with A1 modes (TO3), E (TO4) and another wide band (low intensity) around to 720 cm^{-1} associated with A1 modes (LO3) and E (LO4). When the Mg concentration increases, the peaks at 200 cm^{-1}, 230 cm^{-1} and 290 cm^{-1} in BT tend to merge into a single broad band between 180 cm^{-1} and 290 cm^{-1} in BM_xT.

There is also a decrease in intensity of modes E(TO3 + LO2) / B1, E(TO4) / A1(TO3) and widening of the band E(LO4) / A1(LO3). These are the result of Raman shift frequencies of the modes, but also the presence of a local disorder of the phase that is due to the presence of Mg (Figure 10). The mode E(TO3) around 310 cm^{-1} tends to expand and decrease in intensity indicating a tendency towards pseudo-cubic phase. These results are consistent with those found by Kuo Shou-Yi, Yi-Wen Liao, and Hsieh Wen-Feng (Kuo *et al.,* 2001). The evolution of Raman spectra shows that an increased rate of magnesium causes the displacement of the mode E(LO4) +

A1(LO3) to lower frequencies. It is also noted that the peak intensity varies with the mole fraction of Ba /Mg and especially that of E(LO) + E(TO), which is due to the difference in atomic number between Ba and Mg, indicating the progressive distortion of the tetragonal lattice, and its evolution towards the pseudo-cubic phase. In the $MgTiO_3$, one can observe the existence of active modes of phonons (5Ag + 5Eg), suggesting a short-term ordered structure (Figure 11). Modes A located at 229.9 and 320cm^{-1} correspond to the vibrations of Mg and Ti atoms in their octahedral sites along the z axis. Other Ag modes observed around 400.2, 491.2 and 716.4cm^{-1} are assigned to the vibration of oxygen atoms. The Eg mode located at 290 and 356.5cm^{-1} can be linked to the torsion of the oxygen octahedron with the vibrations of Mg and Ti atoms in parallel to the xy plane. For the mode observed around 488.9 cm^{-1}. Ti and Mg atoms are implicated in the vibration, while the Eg mode around 643.9cm^{-1}, is associated with the Ti-O bond.

Photoluminescence polaron characterization of the BM_xT

The polaron designates the charge carrier occupying the state localized in the potential well is produced by the displacement of atoms from their equilibrium positions in the absence of the charge carried. So the polaron is composed of self-trapped carrier responsible for the deformation and the network structure (Komarneni *et al.,* 1999). Figures 12, 13 and 14 show the photoluminescence spectra of BT and Mg doped BT, observed at room temperature. The $Ba_{1-x}Mg_xTiO_3$ (x= 0; 0.5; 0.10 and 0.15) samples showed no luminescence band (figure 12). For 20% ≤ x ≤ 80% all samples present a large luminescence band centered around 4000 cm^{-1}, the small peak centered around 4500 cm^{-1} is present for pure MT and for all concentrations of Mg (figure 13). Mg doped $BaTiO_3$ (x% = 90) and pure $MgTiO_3$ samples all exhibit a luminescence band with two peaks centered around 4500 cm^{-1} (figure 14).

Conclusion

BM_xT powders were prepared by the sol-gel method, and characterized using XRD, Raman and photoluminescence. XRD patterns revealed the existence of three domains depending on magnesium concentration.

At low concentrations, all samples crystallize in the tetragonal structure, confirming the incorporation of Mg in the structure.

When the Mg content increases, we observed the formation of secondary phases, which is confirmed by Raman studies. For 0.15<x<0.9, the difference in symmetry between the two structures makes difficult the insertion of Mg. on the contrary, the barium even at low concentrations cannot inserted in the phase of rhombohedral symmetry.

REFERENCES

Asiaie, R., W.D. Zhu, S.A. Akbar, P.K. Dutta, 1996. Characterization of submicron particles of tetragonal $BaTiO_3$. Chem. Mater. 8(1), 226-234.

Bouayad, K., S. Sayouri, T. Lamcharfi, M. Ezzejari, D. Mezane, L. Hajji, A. Elghazouali, M. Fillali, P. Dieudonné, and M. Ghouta, 2005. Sol gel processing and dielectric properties of $(Pb_{1-y}La_y)(Zr_{0.52}Ti_{0.48})O_3$, Physica A 358, 175.

Cheng Liu, Peng Liu, Guo-guang Yao, Xiao-bingBian, Hui-xia Jing, Xiao-gang, Lu, Chang-jieGao, 2011. Improvement of dielectric thermal stability of BST ferroelectric material for tunable applications. *Materials Research Bulletin.,* 46, 1510-1514.

Harhira, A. 2007. Thèse de doctorat Photoluminescence polaron dans le niobate de lithium : approche expérimentale et modélisation. Université Paul Verlaine - Metz, Octobre.

Jayanthi, S., T.R.N. Kutty, 2006. Dielectric properties of barium magnesiotitanate ceramics, *Materials Letters*, 60, 796-800.

Kang, S.O., B.H. Park, Y.I. Kim, 2008. Growth mechanism of shape-controlled barium titanate nanostructures through soft chemical reaction. *Cryst. Growth Des.,* 8(9), 3180-3186.

Kellati, M., S. Sayouri, N. Elmouden, M. Elaatmani, A. Kaal, and M. Taibi, Structural and dielectric properties of La-doped lead titanate ceramics, Mater. Res. Bull. 39, 6 (2004).

Komarneni, S., I. Abothu, A. Prasado Rao, 1999. sol-gel processing of some Electroceramic powders. *Sol-Gel Science and Technology,* 15, 263-270.

Kong, L. B., J. Ma, H. Huang, R.F. Zhang, W.X. Que, 2002. Barium titanate derived from mechanochemically activated powders. Alloys and compounds 337, 226-230.

Kuo, S.Y., W.Y. Liao, and W.F. Hsieh, 2001. Structural ordering transition and repulsion of the giant LO-TO splitting in polycrystalline $Ba_xSr_{1-x}TiO_3$, *Physical Review B,* Vol. 64, P. 224103

Ohara, S., A. Kondo, H. Shimoda, K. Sato, H. Abe, Naito, M. Mater, 2008. Rapid mechanochemical synthesis of fine barium titanate nanoparticales Materials Letters, 62, 2957-2959.

Swartz, S.L., T.R. Shrout,W.A. Schulze, L.E. Cross, 1984. *J. Am. Ceram. Soc.,* 67, 311.

Tagantsev, A. K., V. O. Sherman, K. F. Astaviaev, 2004. Ferroelectric Materials for microwave Tunable Applications. *Electroceramics*, 10.

Uchino, K., S. Nomura, L.E. Cross, S.J. Jang, R.E. Newnham, 1980. *J. Appl. Phys.,* 51,1142.

Zimmermann, F., M. Voigt, C. Wei, R. Jakoby, P Wangc, W. Meneskloua, E. Ivers-Tiffée, 2001. Investigation of barium stronsium titanate thick films for tunable phase shifters, *Eurapean Ceramic Society*, 21, 2019-2023.

Zouhairi thèse de doctorat, M. 2013. Propriétés physicochimiques des perovskites diélectriques $Pb(Fe_{1/2}Nb_{1/2})O_3$ (PFN) et $Pb_{1-x}La_xTi_{1-x/4}O_3$ élaborées par voie hydrothermale. USMA FST FES.

Zouhairi, M., O. Elghadraoui, H. Bali, T. Lamcharfi, F Abdi, L. Mrharrab, 2014. *Phys. Chem. News*, 72, 42-48.

****